# ELECTRON-BEAM PROPAGATION IN A REDUCED-DENSITY CHANNEL*

S. J. Czuchlewski, T. J. Kauppila, and L. E. Stout
Los Alamos National Laboratory
P.O. Box 1663
Los Alamos, New Mexico 87544

D. Mitrovich
Albuquerque Mission Research Corporation
1720 Randolph Road, SE
Albuquerque, New Mexico 87106

## Abstract

An experiment is underway to study the atmospheric propagation of the 27-MeV PHERMEX electron beam in a reduced-density channel generated by a $CO_2$ laser.

## Introduction

The concept of using a reduced-density channel (RDC) to aid the propagation of an intense relativistic electron beam through the atmosphere has been discussed in the literature for some time.[1-4] To date, however, experimental[2] and theoretical studies[3-4] of this process have been rather limited. Experimental work has been confined to relatively low-energy electrons (a few MeV) and theoretical calculations have been constrained by the models and approximations that had to be employed. In the present project an extensive set of diagnostics will be used to investigate the propagation of a 27-MeV e-beam in a well-characterized density channel. The results will be compared with the predictions of a state-of-the-art particle-in-cell (PIC) simulation code.

The relativistic e-beam will be generated by PHERMEX, an rf linear accelerator that produces a 4-ns, 27-MeV, 0.7-kA beam.[5] A high-energy $CO_2$ laser will be used to create an RDC in atmospheric-pressure nitrogen that has been lightly doped with $SF_6$. Figure 1 shows a schematic of the experiment. A 1- to 2-m long channel is formed when the $SF_6$ absorbs the 10.6-$\mu$m radiation and, subsequently, heats the surrounding nitrogen. A valve separates the channel test cell, which contains the $SF_6$, from the focusing cell. After the channel has formed (~0.5 ms), the e-beam, which has a diameter of ~1 mm, enters the channel through a thin foil. Diagnostics, such as B-dot loops and a two-dimensional streak camera, will be used to monitor the propagation of the beam.

At the present time, an experimental study of the channel-formation process and a theoretical investigation of the propagation of the PHERMEX beam in a channel have been carried out, and these results will be reported here. The comprehensive propagation experiment awaits scheduling at the PHERMEX facility.

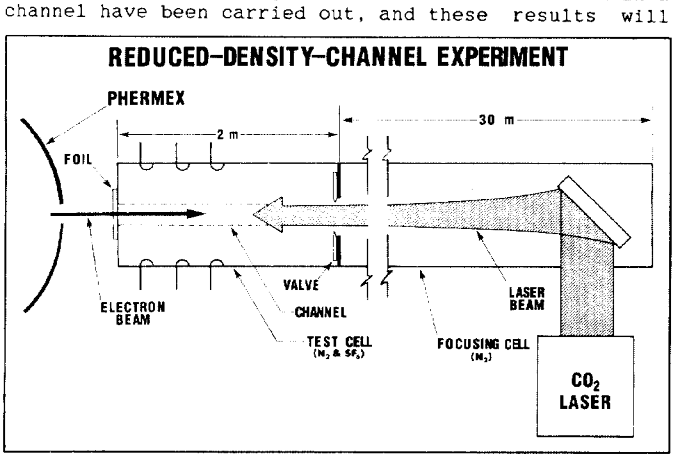


Fig. 1. Schematic of RDC propagation experiment.

*Work performed under the auspices of the U.S. Department of Energy by Los Alamos National Laboratory under W-7405-ENG-36.

## Channel Formation

A commercial e-beam-controlled $CO_2$ laser[6] with an 11 x 11 x 100 $cm^3$ active volume was used in an unstable resonator configuration to generate a 300-J laser pulse. The resonator mirrors were adjusted so that the beam was slightly convergent and came to a focus about 35 m from the laser. The laser pulse consisted of a fast gain-switched spike, followed by a longer main pulse with a duration of 3.6 $\mu$s. To produce a wider channel, a 6.0-cm aperture was inserted in the beam at the laser and only 37% of the output energy was used. This yielded a beam in the test cell that had an approximate Gaussian profile with a characteristic radius of 5.0 mm and a Rayleigh range of ±1.5 m, which are the desired channel dimensions.

To generate a channel, the $N_2$ must be seeded with a gas that absorbs the laser radiation. Ammonia, ethylene, $SF_6$, and $Cl_2C_2F_2$ are among the candidate seed gases; $SF_6$ was chosen because it is the strongest absorber and because the $SF_6$-absorption process has been modeled by workers at NRL.[2,7] If the expansion of the $N_2$ is adiabatic, a deposited energy of ~0.5 $J/cm^3$ is required to produce a 50% reduction in channel density. The NRL model predicted that an $SF_6$ concentration of ~0.2% should be required to achieve this reduction.

As a first step in studying the channels, the transmission of the laser pulse as a function of distance through the $SF_6$ was measured. For 1.2 torr of $SF_6$ in 600 torr of $N_2$ (local atmospheric pressure), transmission data are shown in Fig. 2 along with the predictions of the NRL model.[7] Although the slope of the data appears to be about right out to 100 cm, the predicted energy dependence is not observed. Beyond 100 cm, the slope decreases, which is difficult to explain unless the beam is self-focusing. Nevertheless, it was concluded that the laser photons were being absorbed in a reasonable manner, and it was decided to proceed on to the next step of characterizing the channels that are created by the $CO_2$ laser.

To measure the channel density, the channel was placed in one arm of an interferometer. The displacement of the fringe pattern in the resulting interferogram was a measure of channel depth. An Abel inversion was performed on the interferogram to produce a density profile of the channel as a function of distance from the axis as shown in Fig. 3. Channel depth and width were measured as a function of $SF_6$ concentration, laser energy, and longitudinal position along the channel axis. Figure 3 shows typical density profiles at locations of 17 and 112 cm along the channel for an $SF_6$ partial pressure of 0.8 torr and an incident laser fluence of 51 $J/cm^2$ (a total beam energy of 81 J). It was found that the on-axis densities were reduced to 0.11 and 0.36 of ambient and that channel diameters were 12.4 and 6.2 mm at the two axial locations. The channel extended well beyond the location (z = 112 cm) at which the second interferogram was taken.

TABLE I

CHANNEL DEPTH AND DIAMETER (D) AS A FUNCTION OF AXIAL LOCATION (z) AND $SF_6$ PARTIAL PRESSURE (P) IN 600 TORR of $N_2$

| P (torr) | z = 17 cm $n(o)/n_o$ | D (mm) | 112 cm $n(o)/n_o$ | D (mm) | 165 cm $n(o)/n_o$ | D (mm) |
|---|---|---|---|---|---|---|
| 0.4 | 0.38±.14 | 10.67±.8 | 0.54±.10 | 8.4±.6 | 0.39±.11 | 4.4±1.0 |
| 0.8 | 0.11±.11 | 12.4±1.6 | 0.36 | 6.2±.4 | --- | -- |
| 2.0 | 0.00±.10 | 17.8±1.4 | --- | --- | 0.9 | 1.0 |

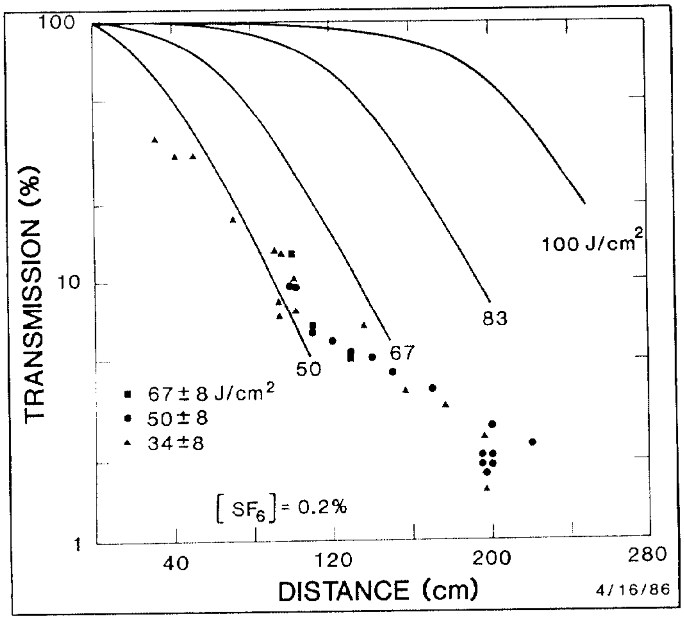


Fig. 2. Transmission of 1.2 torr of $SF_6$ in 600-torr of $N_2$.

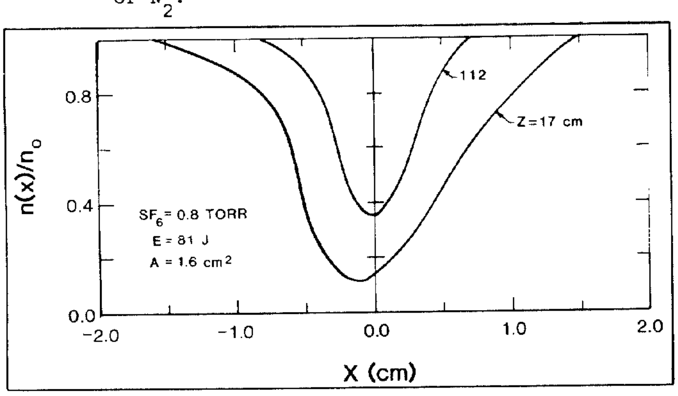


Fig. 3. Channel density profile.

Table I lists measured channel data for several $SF_6$ partial pressures. Incident laser energy was 80 ± 8 J; fluence was 50 J/cm$^2$. It is seen that we can generate either short, deep channels or long, shallow ones. Half-density channels at least 1.6 m in length have been obtained. As expected, near the start of the test cell (z = 17 cm) the channels get deeper as the $SF_6$ concentration is increased. Uncertainty in the densities, computed via the Abel inversion, is ±0.1 of ambient. The channels get narrower as distance increases, reflecting the fact that the laser beam gets narrower as it is absorbed by the $SF_6$. These channels should be adequate to explore e-beam propagation.

## Simulation Studies

Described here are simulation and analytic calculations of the hose behavior of the propagating PHERMEX beam in straight density channels.

The planned experiments use a 700-A, 30-MeV, 4-ns, 1-mm nominal radius beam, which propagates in 580-torr air containing 1-3 torr of $SF_6$ to absorb the laser energy. The laser-heated air column expands, producing a reduced-density channel with a nearly Gaussian profile and a density that can be varied. Being electronegative, the $SF_6$ will remove some of the plasma electrons, decreasing the electrical conductivity. Using $SF_6^-$ reaction-rate data, the BMCHEM code showed that, at the expected $SF_6$ concentrations, the reduction in conductivity was on the order of 1% in the head area of the beam and increased to a modest fraction in the body. Because this change in conductivity was not large, it was not incorporated into the chemistry calculation in IPROP simulations. From the size of the effect, a modest increase in the hose growth rate in the beam body could be attributed to $SF_6$.

The propagation simulations were made using the IPROP particle-in-cell code,[8] with a Gaussian-shaped reduced-density channel aligned with the propagation axis. Channel widths varied from 0.5 cm to ∞, and densities on axis varied between 0.1 and 3 times ambient. For studying linear behavior, only the lowest modes m = 0 and +1 were used. (A separate set of simulations intended to provide direct comparisons of calculated with measured diagnostics was done with modes m = 0, ±1, ±2, ±3, and ±4. These simulations required the largest available CRAY computer at Los Alamos.) The simulations indicated that hose growth in the beam <u>head</u> was fastest at high channel densities, <u>decreasing</u> as channel density was reduced. Hose growth in the beam <u>body</u>, however, was <u>inversely</u> proportional to channel density. Code diagnostics substantiated this conclusion. Figure 4 shows the history of the magnitude of the transverse displacement of a beam slice, from which a hose growth rate can be calculated. This information is summarized in Fig. 5, which shows hose growth rates at different locations in the beam.

The mechanisms controlling hose growth in a density channel were also examined by extending an <u>analytic</u>, linear, rigid-displacement hose-stability model[9] to account for radially varying air density. The model ignores avalanche ionization. From the dispersion relation, the maximum linear temporal hose growth rate is the sum of a growing term, which varies inversely as the transversely-averaged field-dipole decay time $\tau_1$, and of a damping term, which is proportional to the transversely-averaged density and which represents the $k_\beta$ temporal detuning caused by Nordsieck expansion. Because the decay time $\tau_1$ is proportional to conductivity $\sigma$ and because $\sigma$ is small in the beam <u>head</u>, the maximum growth rate there is large and Nordsieck detuning is negligible. In the beam <u>body</u>, where collisional ionization is balanced by recombination, the conductivity is large, so the growing term is small and varies as the square root of the mean density. The Nordsieck damping term can decrease this substantially and, being proportional to the density, causes the growth rate in the body to increase with decreasing density, a result illustrated in the simulations shown in Fig. 5. The model shows that for the case of PHERMEX, the overall effect of the reduced density channel is to decrease the mean density sampled by

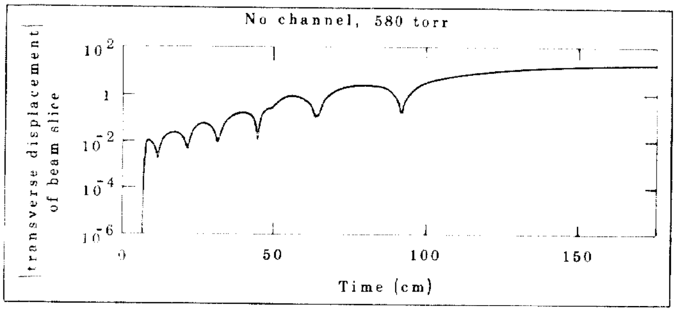

Fig. 4. Beam slice displacement history from IPROP.

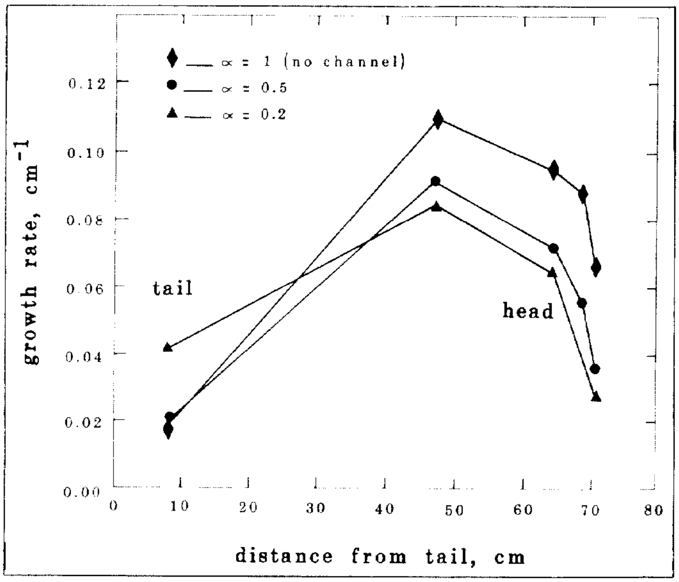

Fig. 5. Linear hose growth rates along the beam.

the beam. No radial gradient effects are seen.

The IPROP simulations demonstrate that as channel density is lowered the decrease of the hose growth rate in the beam head is caused by the increase of conductivity that occurs there from avalanche ionization. For the high-density case the conductivity $\sigma$ in the head region is very small, so the hose growth rate is large. As the channel density is decreased, $\sigma$ in the head increases significantly, lowering the hose growth rate there. When avalanche ionization is turned off, $\sigma$ in the head remains unchanged for the high-density case; however, in the low-density case (deep channel) it decreases dramatically. Thus, in the head the hose growth rate varies inversely with avalanche ionization.

These results are summarized qualitatively in Fig. 6. Hose growth rate in the beam body increases with decreasing channel density because of decreasing Nordsieck damping. In the head, as channel density is reduced, the hose growth rate declines because avalanche ionization increases the conductivity in the head region. With no channel, at 580 torr, hose growth in the head dominates and becomes nonlinear after about 60 cm. At low channel densities hose growth in the body dominates. The hose growth rates are about equal when channel density on axis is about one-half of the ambient 580 torr. Nonlinear behavior in that case starts after about 80 cm of propagation.

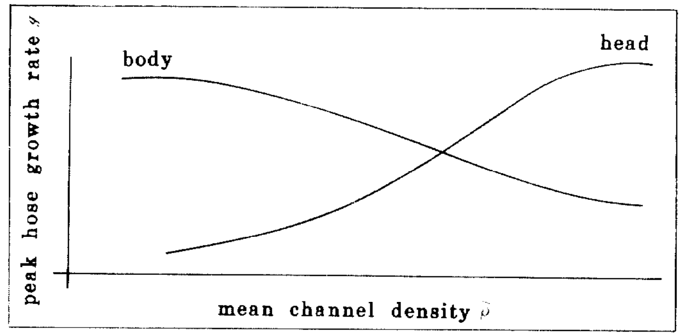

Fig. 6. Qualitative plots of the variation of head and body hose growth rates as functions of mean density.

## Conclusions

Preliminary work on two phases of an experiment to test the propagation of an intense relativistic electron beam has been carried out. It has been demonstrated that appropriate channels (1- to 2-m long with half-ambient density) can be generated with a 75-J $CO_2$ laser. Simulation studies of the beam propagation indicate that the head of the beam will stabilize and that the body will exhibit greater hose instability in the presence of an RDC.

## References

[1] G. A. Askar'yan and N. M. Tarasova, "Passage of Accelerated Particles and Quanta through a Medium Along an RDC Produced by a Laser Beam," JETP Lett. 20, pp. 123-124 (Aug. 1974).

[2] D. P. Murphy, M. Raleigh, R. Pechacek, and J. Greig, "Interaction of an intense REB with preformed channels," Phys. Fluids 30, pp. 232-238 (January 1987).

[3] J. Masamitsu, S. Yu, and F. Chambers, "Beam Tracking Studies with Ringbearer-II," LLNL Report No. UCID-19771 (Nov. 22, 1982).

[4] B. Hui and M. Lampe, "Numerical and Analytical Studies of Beam Channel Tracking," NRL Report No. 5136 (Feb. 29, 1984).

[5] T. P. Starke, "PHERMEX Standing-Wave Linear Electron Accelerator," IEEE Trans. Nuc. Sci. NS-30 (2), pp. 1402-1404 (1983), and D. C. Moir, L. A. Builta, and T. P. Starke, "Time-Resolved Current, Current-Density, and Emittance Measurements of the PHERMEX Electron Beam," IEEE Trans. Nuc. Sci. NS-32 (5), pp. 3018-3020 (October 1985).

[6] K. Manes et al., "Valkyrie: A $CO_2$ Laser System for Laser Fusion Experiments," IEEE J. Quant. Elect. QE-12, pp. 265-273 (1976).

[7] D. Murphy, Naval Research Laboratory, private communication.

[8] B. B. Godfrey, "The IPROP Three-D Beam Propagation Code," Mission Reserach Corporation Report AMRC-R-690 (March 1985).

[9] L. Feinstein, Science Applications International Corporation report SAIC-U-74-PA-DOE, Appendix A (December 1984).